Journal of Engineering Physics and Thermophysics, Vol. 78, No. 6, 2005

EFFECT OF HIGH-CONCENTRATION ENERGY FLUXES ON MATERIALS

DETERMINATION OF THE OPTICAL-BREAKDOWN THRESHOLD UNDER IRRADIATION OF CONDENSED INCLUSIONS BY PULSED LASER RADIATION

K. N. Volkov and V. N. Emel'yanov

UDC 532.529:536.24

On the basis of the thermal approach, a mathematical model of the optical breakdown on condensed inclusions exposed to pulsed laser radiation is developed. As individual stages of the process, we consider the particle heating and evaporation, the formation of a vapor aureole and its ionization, as well as the propagation of shock waves in the space surrounding the particle. The threshold characteristics of the laser-beam parameters sufficient for initiating an optical breakdown on metal and dielectric particles, as well as on dielectric liquid drops are determined.

The presence of particles having fairly low values of the vaporization temperature and ionization potential leads to a decrease in the threshold values of the optical breakdown compared to the breakdown threshold in a pure gas [1, 2]. The search for conditions under which a decrease in the threshold value of the laser-pulse intensity is possible is of interest for both laser initiation of processes and radiation transportation through explosive mixtures.

To construct a model of the laser-radiation interaction with a particle, the explosive and thermal approaches are used. In the first approach, the particle, being inertially attached, during a pulse manages to absorb energy sufficient for its complete evaporation. At high energy concentrations, the particle is heated so fast that the condensed-phase substance acquires the parameters of the overheated metastable state and passes to vapor by way of explosion. The thermal approach is based on a more detailed consideration of such elements of the processes as heating, evaporation, and ionization of the vapor cloud.

The role of explosive evaporation in the decrease in the optical breakdown threshold is discussed in [3]. For solid particles the breakdown mechanisms are realized in the material vapors at $T \sim 10^4$ K. For water droplets with r_p = 50–200 μm the process of explosive evaporation proceeds at lower temperatures $T_v \sim 10^3$ K. As a mechanism initiating optical discharge, the shock waves resulting from the droplet expansion and the high pressure inside it ($p > 10^3$ atm) are considered.

In [4], the explosive mechanism of the laser-radiation interaction with a water droplet is described. Rather long pulses ($t_i \le 300$ μsec) and comparatively large drops (r_p = 100–200 μm) at $Q \sim 1$ J are considered. The explosive evaporation of the droplet is explained by the appearance and growth inside it of vapor bubbles when the liquid temperature reaches the value of the explosive boiling temperature (for water at normal pressure it is equal to 578 K). In [5], the following reasons for the decrease in the breakdown threshold to the values of $I_* = 10^7$–10^8 W/cm^2 in the presence of water droplets are considered:

1. The thermal explosion of the particle, the condition for which is the absorption by the particle of energy exceeding the heat of its evaporation in a time shorter than the time of travel of sound through its cross section.
2. The thermal ionization of the gas on the shock wave arising from the particle explosion.
3. The laser radiation self-focusing inside the particle leading to the formation in its volume of a region of higher energy release. High pressures lead to the formation of shock waves inside the droplet, causing an outflow at the water–air interface, which is a reason for the droplet fragmentation.

D. F. Ustinov Baltic State Technical University "Voenmekh," 1, 1st Krasnoarmeiskaya Str., St. Petersburg, 190005, Russia. Translated from Inzhenerno-Fizicheskii Zhurnal, Vol. 78, No. 6, pp. 106–117, November–December, 2005. Original article submitted February 13, 2004.

1062-0125/05/7806-1155

4. The existence inside the droplet of "hot points" on which the processes of intensive interaction between the radiation and the substance are localized.

In [6], it is noted that on small droplets of water (r_p = 30 μm) the breakdown occurs in two stages. First it arises inside the droplet in the region of its shadow hemisphere. After the plasma site expands and the perturbation comes out from the droplet an air breakdown in the environment is initiated. The internal breakdown is explained by the presence inside the droplet of microscopic polluting particles serving as sites of plasma formation. The expansion velocity of the droplet is estimated to be of the order of 0.6–2 km/sec.

The appearance of primary breakdown sites inside the droplet is a necessary condition for the subsequent development of optical discharge in the gas [7]. At $I < 4 \cdot 10^9$ W/cm^2, a primary breakdown site arises near the back surface of the droplet in the region of the shadow peak of intensity. At $I > 4 \cdot 10^9$ W/cm^2, primary sites are observed in the region of the front-intensity maximum near the front (illuminated) surface of the droplet. As a result of the fast development of the breakdown, the radiation flux sharply attenuates, reaching the shadow peak of intensity, and no breakdown site is formed near the back surface of the droplet.

Systematic presentation of the questions connected with the optical breakdown on condensed inclusions is given in monographs [1, 2]. Primary consideration is given to hard inclusions of the type of corundum, aluminum oxide, and other refractory materials. In many cases, very short pulses are used, which affects the character and specific gravity of all physical processes that proceed.

In the present paper, we propose a mathematical model of the optical breakdown on condensed inclusions (metal and dielectric particles, as well as dielectric liquid droplets) exposed to pulsed laser radiation. The model is based on the concept of the thermal approach [8]. As individual stages of the process, we consider the particle heating and evaporation, the formation of a vapor aureole and its ionization due to the thermal ionization at the shock wave front, and the propagation of shock waves in the space surrounding the particle. The models of the laser-breakdown formation on metal and dielectric particles, as well as on dielectric liquid droplets, differ by the mechanism of the appearance of seed-free electrons and subsequent formation of an electron avalanche. Simulation of the shock-wave processes in the vapor aureole of the particle is carried out on the basis of the nonstationary flow equations of a perfect gas. The threshold characteristics of the laser-beam parameters sufficient for initiating an optical breakdown on condensed inclusions are determined.

The results of the numerical simulation are of interest for determining the threshold power of the laser beam providing inflammation and detonation of the gas-dispersive mixture [9, 10].

Mechanism of Breakdown on Condensed Inclusions. Consider the qualitative picture of the optical breakdown on metal and dielectric particles, as well as on the dielectric liquid droplet.

Mechanism of breakdown on the metal particle. Under the action of the laser radiation the metal particle is heated to high temperatures at which intensive processes of evaporation occur. As a result of the thermionic emission from the particle surface (at $T < T_v$) or the isothermal ionization in the vapor aureole (at $T > T_v$), free electrons are formed. Ionization of the vapor aureole due to the inverse dragging efficiency leads to the formation of an electron avalanche and a microplasma site near the particle. The characteristics of this process depend on both the optical properties of the disperse inclusions and the shape of the particles and their size compared to the radiation wavelength.

Further energy input leads to an expansion of the microplasma sites due to the thermal diffusion of electrons into the regions adjoining the vapor aureole and the inclusion in the ionization process of molecules and atoms of the gas surrounding the particle. The plasma becomes opaque to the radiation, which is completely assimilated by the plasma formation. The pressure increases and the high-temperature region expands, which leads to the formation of a system of shock and acoustic waves propagating in the space surrounding the particle.

The key point of the scheme is the fairly low boiling temperature and the low potential of metal-particle ionization, providing the development of an electron avalanche.

Mechanism of breakdown on the dielectric particle. The factors inhibiting the development of a laser breakdown on dielectric particles as compared to metal particles are the higher values of the ionization potential and the significant local overheating of the gaseous medium.

As mechanisms providing the presence in the system of free electrons, the regions of high parameters in internal vapor bubbles and the regions of the gas heated by the shock waves serve. The gas heating in the immediate

vicinity of the particle surface promotes the appearance of thermal electrons, which leads to the initiation of an electron avalanche and the laser plasma formation.

Mechanism of breakdown on the dielectric liquid droplet. Heating and evaporation of the droplet are delayed because of the weak radiation absorption, and the vapors themselves contain no free electrons in concentrations sufficient for the development of an electron avalanche because of the low evaporation temperature. The dominant role in the development of a laser breakdown is played by the mechanism of explosive evaporation of the particle.

When a transparent particle is exposed to a directed radiation flux, it is focused in the region of the shadow hemisphere of the droplet. In the region of intensive heat release, overheating conditions arise, taking the liquid to the metastable state, in which its temperature exceeds the temperature of saturated vapors at a given temperature. Further energy input leads to the formation of an internal vapor cavity, into which the liquid boils off.

Pressure increase in the bubble creates the conditions for internal breakdown and the appearance of a microplasma site, which, being opaque, intensively absorbs the radiation. An increase in the pressure in the vapor bubble leads to the formation of a shock inside the droplet wave, and the moving of this wave to the interface leads to the appearance of an unloading wave moving inside the droplet and to a marked increase in the liquid particle velocity at the droplet boundary. This causes a release of the substance in the direction of radiation from the back hemisphere of the particle in the form of fine droplets.

The droplet expansion and the moving of the internal shock wave into the environment lead to the development of thermal ionization of the gas at the shock-wave front. The free electrons that have appeared initiate the chain mechanism of breakdown, receiving the electromagnetic field energy due to the inverse dragging effect.

Laser-Pulse Model. The laser-pulse intensity is given in the form

$$I(t, x, y, z) = I_{\max} f_1(t) f_2(x, y) f_3(z) .$$

The change in the pulse intensity with time is modeled by the continuous piecewise-linear function formed on the basis of the real system characteristics [11]. The function modeling the piecewise-linear time dependence of the laser-pulse intensity is written on the system of points t_1, ..., t_N with values F_1, ..., F_N as

$$f_1(t) = \sum_{n=1}^{N-1} \left[F_n + (F_{n+1} - F_n) \frac{t - t_n}{t_{n+1} - t_n} \right] \phi(t_n, t_{n+1}) ,$$

where the function $\phi(t_1, t_2)$ gives a unit step:

$$\phi(t_1, t_2) = \frac{t - t_1 + |t - t_1|}{2|t - t_1| + \delta} - \frac{t - t_2 + |t - t_2|}{2|t - t_2| + \delta} .$$

The small quantity δ is introduced into the denominator to avoid the possible division by zero. The piecewise-linear representation of the laser-pulse shape permits calculating its time characteristic:

$$\Theta = \int_0^\infty f_1(t)\, dt = \frac{1}{2} \sum_{n=1}^{N-1} \frac{F_{n+1} + F_n}{t_{n+1} - t_n} .$$

In the plane normal to the direction of the laser-pulse propagation, the spatial intensity distribution obeys the Gauss law:

$$f_2(x, y) = \exp[-2(x^2 + y^2)/R^2] .$$

The attenuation of the pulse as it passes through the medium is simulated by means of the Bouguer–Lambert–Beer law [1]:

$$f_3(z) = \exp(-\mu z) .$$

The absorption coefficient depends on the nature, state, and concentration of particles, as well as on the transmitted-light wavelength.

The total energy of the laser pulse is related to its intensity and shape by the relation

$$Q = \int_0^\infty \int_0^{2\pi} \int_0^\infty I_{\max} f_1(t) \exp(-2r^2/R^2)\, r dr d\varphi dt ,$$

whose integration yields the formula

$$Q = \frac{\pi}{2} I_{\max} \Theta R^2 ,$$

from which we determine the initial pulse intensity.

Laser Heating Models. Depending on the ratio between the characteristic times of temperature-field transformation inside the particle and the laser beam, models of thermally thin and thick particles are used. In so doing, one should take into account that not all details of the heating dynamics play an equivalent part in determining the threshold conditions of breakdown. Of particular importance seems to be the estimation of the pulse energy providing the onset of developed evaporation of the particle and creating the conditions for ionization of the vapor aureole [1, 2].

Thermally thin particle. The thermally thin particle model is used to describe the heating, melting, and evaporation of metal particles.

It is assumed that at a temperature below the melting point only heating of the particle occurs ($T_p < T_m$). As the melting temperature is reached, the particle completely melts ($T_p = T_m$) and then continues to be heated ($T_p > T_m$). The latent heat of the phase transition solid substance–liquid is ignored. Evaporation is included as an element of the physical process only from the moment the boiling temperature is reached ($T_p \geq T_v$). The evaporation rate is determined by the quantity of energy absorbed by the particle.

The model under consideration includes the equations of:

particle heating to the melting temperature

$$c_p m_{p0} \frac{dT_p}{dt} = K_p I W_{p0} ;$$

particle melting

$$H_m m_{p0} \frac{d\zeta_p}{dt} = K_p I W_{p0} ;$$

particle heating to the boiling temperature

$$c_p m_{p0} \frac{dT_p}{dt} = K_p I W_{p0} + \varepsilon\sigma (T^4 - T_p^4) S_{p0} ;$$

evaporation of the particle

$$H_v \frac{dm_p}{dt} = K_p I W_p + \varepsilon\sigma (T^4 - T_p^4) S_p .$$

The absorption efficiency factor is estimated in terms of the value of the complex refractive index of the medium [1].

Thermally thick particle. Simulation of the heating of the thermally thick particle requires the use of the nonstationary heat-conduction equation. Such a model is used to describe the temperature field in carbon particles and their adjoining space, as well as to heat dielectric liquid droplets, when by virtue of effects described by the Mie theory regions of internal focusing with a higher energy release take place.

In conservative form the heat-conduction equation for the gas ($k = 1$) and the particle ($k = 2$) with regard for the internal heat sources in the spherical coordinate system is written in the following form:

$$\rho_k c_k \frac{\partial T_k}{\partial t} = \frac{1}{r^2}\frac{\partial}{\partial r}\left(r^2 \chi_k \frac{\partial T_k}{\partial r}\right) + G_k(r, t). \quad (1)$$

The terms G_1 and G_2 are associated with the chemical reactions in the mixture and the volume heat release caused by the laser radiation absorption by the particle. The source term G_1 is calculated proceeding from the combustion kinetics of a particular mixture [12]. The energy input intensity per unit volume of the particle is found from the relation

$$G_2 = \frac{IK_{\mathrm{p}}W_{\mathrm{p}}}{V_{\mathrm{p}}}.$$

The condition of thermal conjugation at the boundary of the particle with the gaseous environment (in the absence of the processes of phase transition on its surface or their immateriality) is written as the equation of continuity of thermal fluxes

$$\chi \left.\frac{\partial T}{\partial r}\right|_{r=r_w} - \chi_{\mathrm{p}} \left.\frac{\partial T_{\mathrm{p}}}{\partial r}\right|_{r=r_w} = \mu I(t),$$

which is complemented by the temperature-continuity condition $T_{\mathrm{p}} = T$ at $r = r_w$. In the case of the particle melting at the solid substance–liquid interface, the Stefan condition

$$\chi \left.\frac{\partial T}{\partial r}\right|_{r=r_w} - \chi_{\mathrm{p}} \left.\frac{\partial T_{\mathrm{p}}}{\partial r}\right|_{r=r_w} = \rho_{\mathrm{p}} H_{\mathrm{m}} u_{\mathrm{m}}$$

is fulfilled. In the presence of evaporation, the boundary condition on the particle surface has the following form:

$$\chi \left.\frac{\partial T}{\partial r}\right|_{r=r_w} = \rho H_{\mathrm{v}} u_{\mathrm{v}} - \mu I.$$

To describe the particle evaporation that occurs in the region of time-variable size the coordinate system connected with the particle surface is used. In using the new coordinate

$$\eta = \frac{r}{r_w(t)}$$

Eq. (1) at a constant heat-conductivity coefficient acquires the form

$$\rho_k c_k \left(\frac{\partial T_k}{\partial t} - \frac{\eta}{r_w^2}\frac{dr_w}{dt}\frac{\partial T_k}{\partial \eta}\right) = \frac{\chi_k}{r_w^2}\left(\frac{\partial^2 T_k}{\partial \eta^2} + \frac{2}{\eta}\frac{\partial T_k}{\partial \eta}\right) + G_k(\eta, t). \quad (2)$$

Eq. (2) is solved by the finite-difference method.

Internal vapor cavity droplet. At a volume heat input to the drop, its central regions are superheated and the liquid in them is in the metastable state [13]. In this case, a vapor cavity can be formed inside the droplet, and the boiling off of the liquid into it causes a pressure increase, cavity expansion, and vapor explosion of the droplet.

If the liquid flow inside the droplet is considered to be spherically symmetric and potential, then the dynamics equation of a droplet with an internal gas cavity represents the generalization of the Rayleigh equation for the gas-cavity motion in an unlimited fluid [14]:

$$\left(1 + \frac{r_{\mathrm{b}}}{r_w}\right)(r_{\mathrm{b}}\ddot{r}_{\mathrm{b}} + 2\dot{r}_{\mathrm{b}}^2) - \frac{1}{2}\left(1 + \frac{r_{\mathrm{b}}^4}{r_w^4}\right)\dot{r}_{\mathrm{b}}^2 = \frac{p_{\mathrm{b}} - p_w}{\rho / r_w},$$

where p_w and p_b are the pressures at the outer boundary of the droplet (at $r = r_w$) and on the gas-cavity surface (at $r = r_b$).

Closing relations. To calculate the pressure of saturated vapors over the liquid-phase surface, the Clausius–Clapeyron equation is used [13].

Under equilibrium evaporation conditions, the whole of the heat absorbed by the particle is assimilated in the process of phase transitions, whose intensity is determined by the latent heat of evaporation. The balance energy relation has the form

$$-4\pi r_w^2 \chi_p \left.\frac{\partial T_p}{\partial r}\right|_{r=r_w} = 4\pi r_w^2 \rho_p H_v \frac{dr_w}{dt}.$$

Passing to the dimensionless coordinate connected with the variable particle radius, we obtain the relation

$$\frac{dr_w^2}{dt} = -\frac{2\chi_p}{\rho_p H_v} \left.\frac{\partial T_p}{\partial \eta}\right|_{\eta=1} \tag{3}$$

for determining the current size of the droplet being evaporated.

Under nonequilibrium conditions, the relations obtained for the equilibrium regime are usually used, but with proper corrections. In particular, it is assumed that the transition of the superheated liquid to the vapor phase begins (at such superheating temperatures) when in this liquid a quantity of heat equal to the doubled heat of the phase transition has been accumulated [13].

Vapor Aureole Ionization Model. For the given range of parameters, the mechanism of laser plasma formation is associated with the radiation pumping into the electronic component due to the inverse dragging effect. The other mechanisms of plasma formation, in particular, multiphoton ionization, are not determining [15, 16]. The mathematical model incorporates the following equations:

$$\frac{dT_a}{dt} = \frac{6m_e}{5m_a}(T_e - T_a)\,\alpha\nu,$$

$$\frac{dT_e}{dt} = -\left(T_e + \frac{2E}{5k}\right)\frac{1}{\alpha}\frac{d\alpha}{dt} - \frac{6m_e}{5m_a}(T_e - T_a)\,\nu + \frac{2}{5k}\frac{\mu I}{\alpha n},$$

$$\frac{d\alpha}{dt} = \frac{A}{T_e^{9/2}} n \left[\alpha(1-\alpha)\frac{\beta^2 n}{1-\beta} - \alpha^3 n\right],$$

$$\frac{dm_p}{dt} = -\frac{K_p I W_p}{H_v}.$$

Here $A = 1.05 \cdot 10^{-8}$ cm$^6 \cdot$K$^{9/2}$. The equilibrium degree of ionization of metal vapors is determined from the Saha equation at evaporation temperature. To close the above equations, the relations given in [8, 15] are used.

Because the induction period of the chemical reaction is comparable in time to the laser-pulse duration, no substantial energy contribution is expected from the chemical reaction during the laser action. This makes it possible, as the first approximation, not to solve the energy equation for the gaseous component during the laser irradiation, but to find the mixture parameters from the simplified model on the assumption of adiabatic compression of the mixture of aureole vapors.

The specific feature of the problem of the radiation interaction with dielectric particles is the absence of mechanisms providing the presence in the system of a sufficient number of free electrons. As processes supplying the electronic component, the regions of high parameters in internal vapor cavities and the regions of shock-wave-heated gas act.

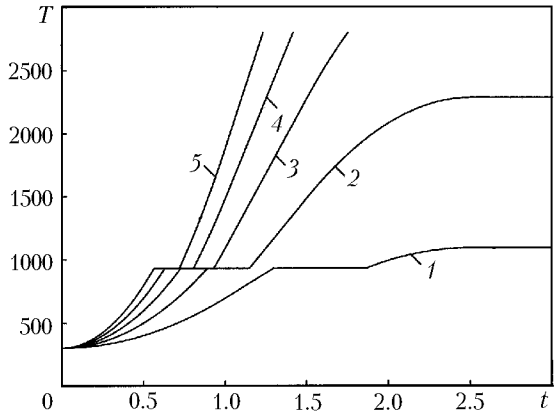

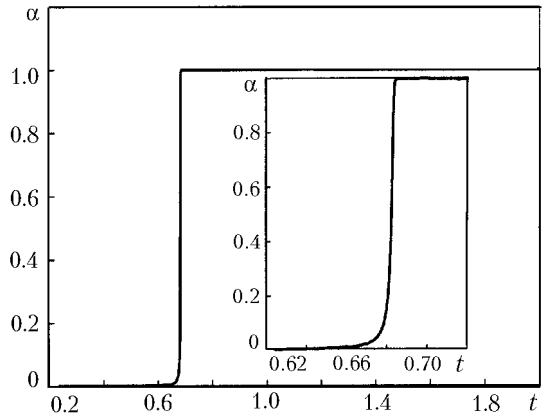

Fig. 1. Temperature in heating of the aluminum particle by the laser radiation to the boiling temperature depending on the laser-pulse power: 1) Q = 1; 2) 2; 3) 3; 4) 4; 5) 5 J. T, K; t, μsec.

Fig. 2. Time dependence of the degree of ionization of aluminum vapors at Q = 1.5 J. t, μsec.

Gas-Dynamic Processes in the Vapor Aureole. Simulation of the gas-dynamic processes in the vapor aureole of the particle is reduced to the integration of the nonstationary perfect gas flow equations. In vector form the conservation laws have the form

$$\frac{dm_{\mathrm{p}}}{dt} = -\frac{K_{\mathrm{p}} I W_{\mathrm{p}}}{H_{\mathrm{v}}}.$$

$$\frac{\partial \mathbf{U}}{\partial t} + \frac{\partial \mathbf{F}(\mathbf{U})}{\partial x} = \mathbf{G}. \tag{4}$$

The vector of gas-dynamic variables, the flux vector, and the source term are found as

$$\mathbf{U} = \begin{pmatrix} \rho \\ \rho u \\ \rho e \\ \rho Y_j \end{pmatrix}, \quad \mathbf{F} = \begin{pmatrix} \rho u \\ \rho u^2 + p \\ (\rho e + p)\, u \\ \rho Y_j u \end{pmatrix}, \quad \mathbf{G} = \begin{pmatrix} 0 \\ 0 \\ 0 \\ \omega_j \end{pmatrix}.$$

Equation (4) is closed by means of the caloric and thermal equations of state. The rate of change in the mass concentration of the jth component of the mixture is calculated depending on the combustion kinetics of a particular chemical composition [12].

For discretization of Eq. (4) the control volume approach and the idea of splitting into physical processes are used. The fluxes are calculated using the Godunov–Kolgan scheme [17].

Results of the Calculations. As a radiator, we use a pulsed chemical HF laser having the following characteristics [11]: t_{i} = 2.6 μsec; λ = 4.2 μm; R = 1.5 cm; θ = 1.5 μsec. The thermophysical and optical properties of particles were taken from reference books with allowance for their temperature dependence.

Metal particle. Aluminum particles irradiated by a laser pulse have a lamellar form and are represented in the model as plates of size 5 × 50 × 50 μm.

The particle temperature depends on the laser-pulse power. The computational model fairly well describes the phase transition associated with the particle melting (Fig. 1). Heating of the particle to the boiling temperature and the evaporation processes that follow strongly depend on its position. Particles that are peripheral with respect to the beam axis do not go to the regime of developed vapor formation and do not create conditions for the start of the plasma-formation process.

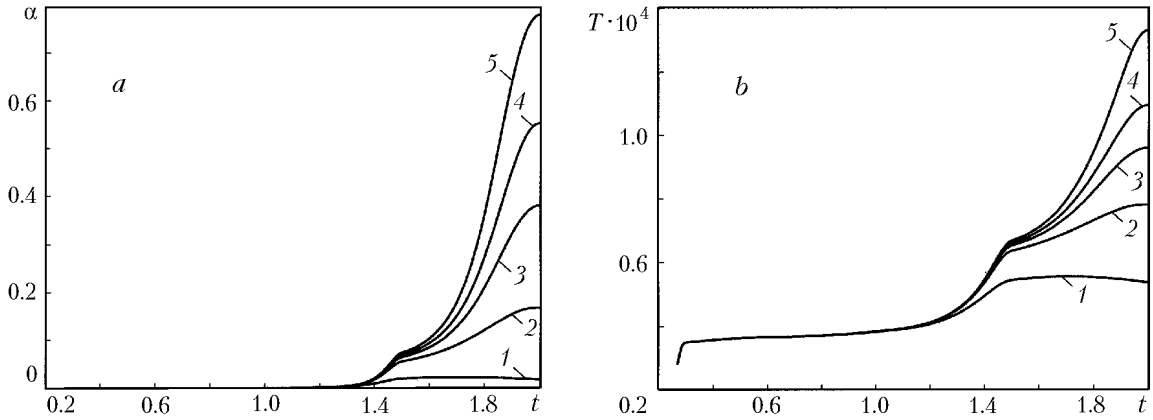

Fig. 3. Change in the degree of ionization of aluminum vapors (a) and in the electronic component temperature (b) with time in the case of the action of a pulse of prebreakdown power: 1) Q = 1.026; 2) 1.027; 3) 1.028; 4) 1.0285; 5) 1.0288 J. T, K; t, μsec.

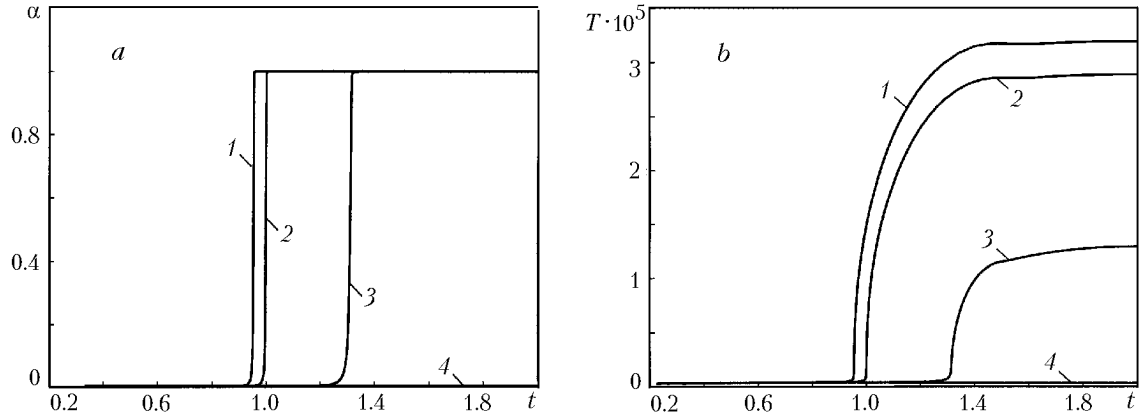

Fig. 4. Dependence of the degree of ionization of aluminum vapors (a) and the electronic-component temperature (b) on the particle position relative to the beam axis: 1) r/R = 0; 2) 0.2; 3) 0.4; 4) 0.5. T, K; t, μsec.

The dynamics of the electron avalanche development is given in Fig. 2 as the time dependence of single ionization of aluminum vapors at Q = 1.5 J. The particle is situated on the beam axis. The evaporation nonequilibrium is modeled by introducing a degree of superheating of the order of 10%. The electron avalanche (see the fragment of Fig. 2) develops 0.68 μsec after the pulse onset. Ionization processes proceed in a short time (of the order of 0.04 μsec). The energy threshold of plasma formation is determined by the portion of the energy transmitted prior to the breakdown onset, which is $Q_* = 16.7$ J/cm^2. The energy characteristic of the breakdown assigned to the energy that falls within the focusing spot accounts for about one-half of the total laser-pulse energy.

The change in the degree of ionization of vapors and in the electronic-component temperature in the case of energy of prebreakdown power of the pulse is shown in Fig. 3. The total energy needed for laser plasma to arise is equal to 1.03 J, and the prebreakdown conditions are fairly sensitive to a small change in the pulse power.

The influence of the particle displacement from the beam axis on the breakdown characteristics is shown in Fig. 4 at Q = 1.5 J. Since the radiation intensity changes depending on the distance from the beam axis by the Gauss law, different times of breakdown onset take place, and for the particle farthest from the axis the breakdown conditions are not realized.

The scaly aluminum particles introduced into the medium can take different orientations in the space. From the point of view of the geometrical optics model, we investigated the influence of the angle between the normal to the main surface of a scale and the direction of the incident radiation on the breakdown energy (Fig. 5). The results

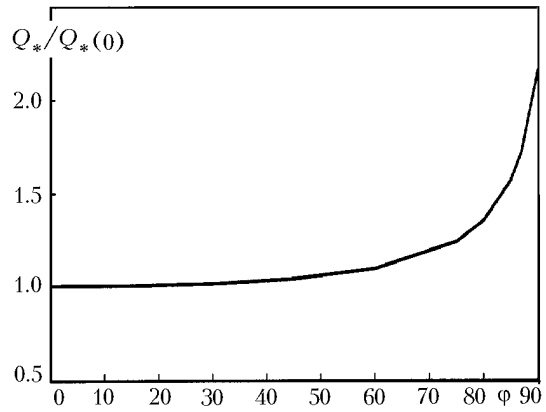

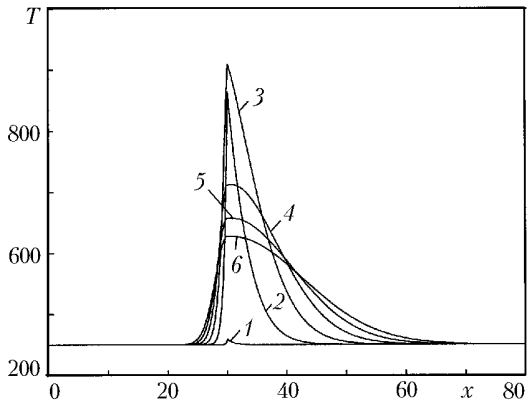

Fig. 5. Ratio of the breakdown energy to the breakdown energy at a zero angle between the normal to the particle surface and the laser beam versus the particle rotation angle. φ, deg.

Fig. 6. Temperature field near the graphite particle at Q = 2.5 J. The curves correspond to different instants of time: 1) t = 0.05; 2) 1.09; 3) 2.13; 4) 3.17; 5) 4.21; 6) 5.25 μsec. T, K; x, μm.

of the calculations are normalized to the value of the breakdown energy at $\varphi = 0^o$. The rotation angle influences the effective area absorbing the radiation. The case where the scale is pointed with its lateral face toward the radiation source is the most unfavorable and requires about twice as much energy for the breakdown to arise. At the same time, deviations of the particles by angles up to 60^o do not lead to marked changes in the breakdown threshold.

Dielectric particle. The heating of the dielectric particle is considered from the viewpoint of the distributed model in the plane symmetry approximation. The temperature distribution inside a graphite plate of thickness 10 μm and in the methane–air medium surrounding the particle is given in Fig. 6. The particle is in the range of $20 \le x \le 30$ μm. To calculate the combustion kinetics of methane, the model of [12] was used. At the particle boundary there is a local temperature increase associated with the incident energy flux. As the process is developed, there is a sharp increase in the particle-surface temperature on its side facing the radiation source (the radiation flux is incident on the particle from right to left). During the pulse action the particle-surface temperature increases (curves 1, 2), reaches its maximum value by the end of the pulse (curve 3), and upon termination of the pulse action decreases due to the heat transfer from the particle to the environment (curves 4–6).

The energy threshold of the breakdown for graphite particles is an order of magnitude higher than the value obtained for the breakdown realization on metal particles. The increase in the breakdown threshold for graphite particles is due to the increased (almost doubled) ionization potential and the higher temperature at which vapors respond to the ambient pressure. Taking account of these factors in the laser-breakdown model leads to threshold values exceeding the breakdown threshold on the metal particle by a factor of about 2.5.

Dielectric liquid droplet. To determine the threshold breakdown conditions, we sequentially solved the problems of droplet heating to the explosive transformation temperature, shock-wave formation from explosion products, determining the initial concentration of electrons in the gas due to the thermal ionization after the shock-wave front, and development of an electron avalanche in the vapor aureole. The model was corrected by introducing a different value of the ionization potential and using the real gas model for calculating the initial degree of ionization [18].

The temperature field inside the dielectric liquid droplet and in the gaseous medium surrounding it is shown in Fig. 7 (it is assumed that R = 5 mm). Near the droplet a thin boundary heated layer is formed. In the boundary layer of the droplet, the gaseous-medium temperature is rather high, and in this region ionization processes are probable. The heat-release maximum falls within the central regions of the particle.

As, in the region of maximal heat release, the volume boiling condition is reached, a gas cavity is formed inside the droplet. At high energy values in the gas cavity, the conditions for thermal ionization of the gas and initiation of an electron avalanche are created. Owing to the volume heat release, the droplet is superheated and is in the me-

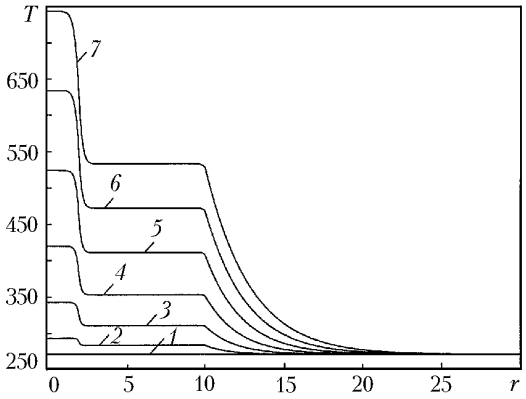

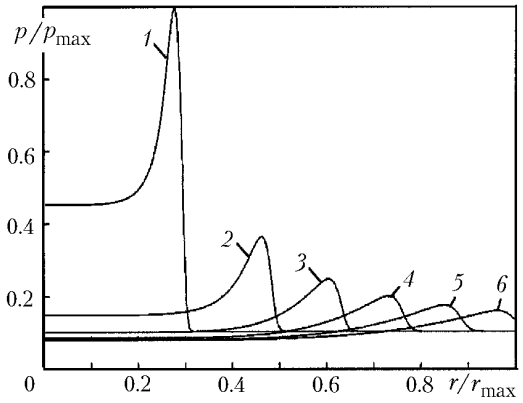

Fig. 7. Temperature field near the dielectric liquid droplet at Q = 20 J. The curves correspond to different instants of time: 1) t = 0.05; 2) 0.30; 3) 0.55; 4) 0.80; 5) 1.05; 6) 1.30; 7) 1.55 μsec. T, K; r, μm.

Fig. 8. Pressure distribution in the vapor aureole of the particle at different instants of time upon termination of the laser-pulse action. The curves correspond to different instants of time: 1) t = 2.60; 2) 2.75; 3) 2.90; 4) 3.05; 5) 3.20; 6) 3.35 μsec.

tastable state. Curve 7 corresponds to the condition of the onset of the explosive process (the explosive transformation temperature is about 698 K, and its time is about 1.54 μsec).

The plasma formation becomes practically nontransparent for the radiation, which leads to an increase in the temperature and pressure of evaporation products, as well as to the formation of a nonstationary gas-dynamic flow in the vicinity of the microplasma formation. The problem was solved in terms of spherical symmetry. Expansion of the laser-plasma formation generates a strong shock wave, whose intensity decreases with increasing distance from the particle center (Fig. 8).

The plasma-formation process is limited by the time of droplet heating to the temperature of explosive transformation (at low pulse energies large droplets have no time to get heated, and small ones intensively exchange heat with the environment), the shock-wave intensity promoting thermal ionization of the gas (for massive drops it is low), and by the electron avalanche development. The appearance of a breakdown is a consequence of the competition between the above factors.

On a droplet of r_p = 5 μm a breakdown is realized at energy $Q_* \sim$ 10 J. As the size of the droplet increases, the time of its heating increases and the degree of ionization after the shock wave decreases. However, the value of Q_* = 15 J is sufficient, according to the calculated estimates, for laser-breakdown initiation. At r_p = 20 μm, there is a decrease in the value of the initial degree of ionization after the shock wave. This leads to the fact that for small laser-pulse energies the electron avalanche does not develop, and the plasma formation threshold increases to Q_* = 30 J.

CONCLUSIONS

1. We have constructed mathematical models of the elementary stages of the process of optical breakdown on condensed inclusions, among which are particle heating and evaporation, vapor aureole formation, the appearance of free electrons due to the thermal ionization at the shock-wave front, and development of an electron avalanche and gas-dynamic processes in both the region of the seed particle and the space surrounding the particle. The threshold characteristics of the laser-pulse parameters sufficient for optical-breakdown initiation have been determined.

2. The data presented show that the proposed mathematical model is informative enough for estimating the threshold characteristics of the optical breakdown. The adopted scheme of the appearance of an electron avalanche on seed electrons formed as a result of thermal ionization on the shock wave explains the qualitative picture of the process and serves as the basis for quantitative assessments. The use of experimental data will make it possible to correct the model and increase the reliability of forecasts obtained on its basis.

NOTATION

A, proportionality coefficient, $m^6 \cdot K^{9/2}$; *c*, heat capacity, J/(kg·K); *e*, total energy of mass unit, J/kg; *E*, ionization potential, J; f_1, function describing the change in the pulse intensity with time; f_2, function describing the spatial distribution of the pulse intensity; f_3, function describing the pulse attenuation as it passes through the medium; *F*, value of the function f_1 at some instant of time; **F**, flux vector; *G*, source term in the heat-conduction equation; **G**, source term; *H*, specific heat of the phase transition, J/kg; *I*, laser-pulse intensity, W/m^2; *k*, Boltzmann constant, J/K; *K*, radiation absorption efficiency factor; *m*, mass, kg; *n*, concentration of heavy particles, $1/m^3$; *N*, number of linear sections on the curve of change in the pulse intensity with time; *p*, pressure, Pa; *Q*, total energy of the laser pulse, J; *r*, radius, m; *R*, characteristic radius of the laser spot, m; *S*, area, m^2; *t*, time, sec; *T*, temperature, K; *x*, *y*, *z*, spatial coordinates, m; *Y*, mass concentration of a mixture component; *u*, velocity, m/sec; **U**, vector of unknowns; *V*, volume, m^3; *W*, effective section area, m^2; α, degree of ionization; β, equilibrium degree of ionization; δ, small quantity; ε, emissivity factor of the particle surface; ζ, relative fraction of melt; η, dimensionless spatial coordinate; Θ, integral time characteristic of the laser pulse, sec; λ, wavelength, m; μ, radiation absorption coefficient, 1/m; ν, frequency of collisions of electrons with atoms and ions, 1/sec; ρ, density, kg/m^3; σ, Stefan–Boltzmann constant, $W/(m^2 \cdot K^4)$; ϕ, function giving a unit step; φ, polar angle; χ, heat conductivity, W/(m·K); ω, chemical reaction rate, 1/sec. Subscripts: a, atom; b, vapor cavity; e, electron; i, laser pulse; *j*, mixture component; *k*, phase of the system; m, melting; max, maximum; p, particle; v, evaporation; *w*, interface; 0, initial instant of time; *, threshold value of a parameter; point, time derivative.

REFERENCES

1. V. E. Zuev, Yu. D. Kopytin, and A. V. Kuzikovskii, *Nonlinear Optical Effects in Aerosols* [in Russian], Nauka, Novosibirsk (1980).
2. Yu. D. Kopytin, Yu. M. Sorokin, A. M. Skripkin, N. N. Belov, and V. I. Bukatyi, *Optical Discharge in Aerosols* [in Russian], Nauka, Novosibirsk (1990).
3. A. A. Zemlyanov, A. V. Kuzikovskii, and L. K. Chistyakova, On the mechanism of optical breakdown under irradiation of water targets by the radiation from a pulsed CO_2 laser, *Zh. Tekh. Fiz.*, **51**, Issue 7, 1439–1444 (1981).
4. V. S. Loskutov and G. M. Strelkova, On explosive evaporation of a water droplet under the action of laser pulses at 1.06 and 2.36 μm, *Opt. Spektrosk.*, **53**, No. 5, 888–892 (1982).
5. V. A. Pogodaev and A. E. Rozhdestvenskii, Explosion and optical breakdown of weakly absorbing water aerosols in a strong light field, *Zh. Tekh. Fiz.*, **53**, Issue 8, 1541–1546 (1984).
6. V. K. Mamonov, Experimental study of the kinetics of the development of air breakdown near droplets of weakly absorbing aerosol, *Zh. Tekh. Fiz.*, **55**, Issue 12, 2333–2339 (1985).
7. V. K. Mamonov, Experimental study of the appearance and development of an optical discharge wave at a breakdown in water droplets, *Zh. Tekh. Fiz.*, **56**, Issue 12, 2410–2412 (1986).
8. K. N. Volkov, V. N. Emel'yanov, and Li Sulun, Heat and mass transfer in gas-disperse systems exposed to intense radiation, in: *Proc. IV Minsk Int. Forum "Heat and Mass Transfer–MIF-2000"* [in Russian], Vol. 6, 22–26 May 2000, Minsk (2000), pp. 213–222.
9. K. N. Volkov and V. N. Emel'yanov, Development of heat-transfer and shock-wave processes in two-phase systems under the action of intense radiation fluxes, in: *Proc. III Russian Nat. Conf. on Heat Transfer* [in Russian], Vol. 6, 22–25 October 2002, Izd. MEI, Moscow (2002), pp. 242–245.
10. K. N. Volkov and V. N. Emel'yanov, Interaction between intense radiation fluxes and gas-disperse systems, *Mat. Modelir.*, **15**, No. 6, 35–40 (2003).
11. M. A. Azarov, V. A. Drozdov, V. I. Igoshin, A. Yu. Kurov, A. L. Petrov, S. Yu. Pichugin, and G. A. Troshchinenko, Formation and experimental study of the gas-dispersive medium of a pulsed chemical H_2–F_2 laser initiated by IR radiation, *Kvantovaya Élektron.*, **24**, No. 11, 983–986 (1997).
12. L. S. Polak (Ed.), *Use of Computational Mathematics in Chemical and Physical Kinetics* [in Russian], Nauka, Moscow (1969).

13. V. P. Skripov, *Metastable Fluid* [in Russian], Nauka, Moscow (1972).
14. R. I. Nigmatulin, *Dynamics of Multiphase Media* [in Russian], Pt. 1, Nauka, Moscow (1987).
15. N. I. Koroteev and I. L. Shumai, *Physics of Powerful Laser Radiation* [in Russian], Nauka, Moscow (1991).
16. H. Kopecek, H. Maier, G. Reider, F. Winter, and E. Winther, Laser ignition of methane–air mixtures at high pressures, *Exp. Thermal Fluid Sci.*, **27**, 499–503 (2003).
17. V. P. Kolgan, Application of the principle of minimum values of the derivative to the construction of finite-difference schemes for calculating discontinuous solutions of gas dynamics, *Uch. Zap. TsAGI*, **3**, No. 6, 68–72 (1972).
18. A. N. Kraiko, Analytic presentation of the thermodynamic functions of air, *Inzh. Zh.*, **4**, Issue 3, 548–550 (1964).